Materials Letters 316 (2022) 131970

Contents lists available at ScienceDirect

Materials Letters

journal homepage: www.elsevier.com/locate/matlet

Effect of annealing on irradiation resistance of $(FeCoNi)_{86}Al_7Ti_7$ high entropy alloys

Han Li, Yongkun Mu, Gang Wang, Yandong Jia *, Runzhong Wang

Institute of Materials, Shanghai University, Shanghai 200444, China

ARTICLE INFO

Keywords:
High entropy alloys
Additive manufacturing
Nuclear materials

ABSTRACT

$(FeCoNi)_{86}Al_7Ti_7$ High-entropy alloys show high hardness, fatigue resistance and excellent mechanical property, making it appealing for nuclear industry application. In this paper, $(FeCoNi)_{86}Al_7Ti_7$ High-entropy alloys were fabricated using a selective laser melting technique (SLM). The microstructural evolution of original and annealed the SLM alloys were discussed in detail after irradiating. In addition, the influences of the strength and hardness of high entropy alloys were also investigated.

1. Introduction

High-entropy alloys (HEAs) are newly emerging advanced materials, which are defined as a multi-element solid solution composed of four or more principal elements in equimolar or near-equimolar ratios [1]. HEAs can exhibit high hardness, fatigue resistance, wear resistance and excellent low temperature fracture-resistance [2]. Due to their excellent mechanical properties and high temperature stability, HEAs have been proposed as structural materials in advanced nuclear systems [3,4], in which structural materials will be exposed to high temperatures and high irradiation doses.

HEAs are generally synthesized by the arc-melting and casting process. This fabrication route is unlikely to present an industrially suitable way for the production and use of HEAs, since it is difficult to produce HEA component with complex shape. More importantly, the low cooling rates (10–20 K/s) duloop the conventional casting of HEAs in a crucible would result in strong phase separation [5].With this in mind, it would appear that the selective laser melting technique (SLM), which facilitates complex-part production and generates rapid solidification cooling rates, may be suitable for the fabrication of HEAs [6]. The cooling rates achieved by method can generally reach the values on the order of 10^3–10^4 K/s. In addition, SLM is a near-net shape manufactuloop process, potentially ensuloop the fabrication of HEA component with complex geometry [7].

2. Experimental details

The $(FeCoNi)_{86}Al_7Ti_7$ high entropy alloys were manufactured by SLM device on HBD-100 metal 3D printer. Then the samples were aging annealed in 780 ℃ and kept for 4 h. Then the original and annealed alloys were used as the targets of irradiation experiment. The irradiation experiment were carried out on LC16B special ion implanter at the University of Wuhan. The implanted ion was selected as He^+ ion and the irradiation dose was 2×10^{17} ions/cm^2. The peak of He^+ ion concentration in alloys appears near 400 nm from the irradiation surface, and the peak of irradiation damage can reach 2.5 dpa. There are four samples will be tested by characterization methods with nanoindentation and TEM. The original alloys sample before and after irradiated referred to sample 1 and 2. As well as the annealed alloys samples before and after irradiated by He^+ ions referred to sample 3 and 4.

3. Results and discussion

Fig. 1 shows the relationship between the nanohardness values and indentation depths of the unirradiated and irradiated samples. It is observed that the nanohardness values increased after irradiation for the original alloys, while the phenomenon of irradiation hardening occurs. The nanohardness values of the annealed alloys decreased after irradiation. And here was no irradiation hardening phenomenon, indicating that annealing treatment can inhibit irradiation hardening phenomenon. Finally, for both samples, the nanohardness value went down with an increase in the indentation depth. This is well elucidated by the Nix-Gao model [8]. It can be seen from Fig. 1 that the nanohardness decreased with the increase of indentation depth, which is in line with this calculation model.

* Corresponding author.
E-mail address: yandongjia@shu.edu.cn (Y. Jia).

https://doi.org/10.1016/j.matlet.2022.131970
Received 18 January 2022; Accepted 23 February 2022
Available online 26 February 2022

$$H = H_0\left(1 + \frac{h^*}{h}\right)^{\frac{1}{2}} \quad (1)$$

Fig. 2(a) and (b) combine the SRIM simulation results with the TEM images of the irradiation damage peak region of the irradiated original and annealed alloys samples respectively. The red line is the displacement per atom and the blue line is the concentration distribution of incident He^{2+} ions. As can be seen from Fig. 2, a large number of dislocation loops appear in the area of peak damage. In the process of ion irradiation, a large number of point defects are formed by cascade collision. These point defects collide with each other in diffusion process, resulting in the disappearance of them and the point defect clusters generate. Point defect clusters include gap clusters and vacancy clusters. Because the migration activation energy of gap defects is lower than that of vacancy. It is generally believed that interstitial dislocation loops preferentially nucleate and grow by absorbing interstitial atoms. Chen et al. [9] also observed similar interstitial dislocation loops in Ni based alloys irradiated by He^+ ions. Therefore, it is inferred that the dislocation loops observed in our project are interstitial dislocation loops. From the surface to the interior, the size of the dislocation loops decreases and the density increases.

A number of helium bubbles can be observed in the peak damage area. This region is zoomed further and presented in under-focus and over-focus conditions at Fig. 3 for better identification. As helium bubbles appear as white dots in the under-focus condition as Fig. 3(a) whereas black dots under the over-focus condition in Fig. 3(b). Therefore, through the above comparison between under-focus and over-focus image, it can be judged that these nano-sized white spots are helium bubbles formed by the aggregation of He atoms. From the surface to the interior, the size of the helium bubbles also gradually decreases and the density increases. This is same as the variation law of dislocation loops.

The size and number of dislocation loops and helium bubbles are counted by nanomeasurer software, the size of dislocation loops in the irradiation peak region of the original sample is mostly between 10 and 19 nm, accounting for more than 80% of the total. The dislocation loops size in the irradiation peak region of annealed sample is usually between 8 and 12 nm, and some dislocation loops can reach 13.5–21 nm. For the original sample, the average size of dislocation loops is 13.83 nm and the number density is 1.38×10^{22} m^{-3}. For the annealed sample, the average size of dislocation loops is 10.96 nm and the number density is 2.77×10^{22} m^{-3}. The number density of dislocation loops in the original alloys are approximately twice that in the annealed alloys. Therefore, we get that the density of dislocation loops in the original sample is less than that in the annealed sample, but its size is much larger than that in the annealed sample.

The helium bubble size in the irradiation peak region of the original sample is between 1.2 and 2 nm. The helium bubble size in annealed sample is between 0.9 and 1.5 nm. The statistical results show that the average size of helium bubbles in the original sample is 1.67 nm and the number density is 9.6×10^{23} m^{-3}. The average size of helium bubbles in annealed samples is 1.25 nm and the number density is 1.45×10^{24} m^{-3}. In the meanwhile, It is found that the density of helium bubble in the original sample is less than that in the annealed sample, but its size is larger than that in the annealed sample.

The statistical results show that the size and number density of dislocation loops have the same trend as that of helium bubbles. Trinkaus et al. [10] mentioned that the formation mechanism of helium bubbles is controlled by He redissolution or dissociation. He atoms decompose from helium bubbles through displacement, resulting in the reduction of helium bubble size; Generally helium bubble density increases and the size decreases with the increase of He production rate. The variation trend of helium bubble size and number density obtained in our project is just in line with the nucleation mechanism of helium bubble.

TEM results show that the irradiated samples produced nano-sized dislocation loops and helium bubbles. According to previous reports on hardness of alloys irradiated by He ion, point defects such as helium bubbles and dislocation loops are dispersed in the alloy matrix, pinning dislocations and preventing the free movement of dislocation lines, resulting in the increase of yield strength and the hardness of materials also increased [11]. Increase in yield strength ($\Delta\sigma_y$) due to defects. It can be estimated according to the DBH model [12]

$$\Delta\sigma y = \alpha M \mu b (ND)^{\frac{1}{2}} \quad (2)$$

A large number of nano-sized dislocation loops and helium bubbles were produced in the irradiated original samples and annealed samples, while there were no such defects in the non irradiated samples except dislocation lines. Therefore, it can be inferred that the hardening of FeCoNiAlTi high entropy alloys samples after irradiation is mainly caused by defects such as helium bubbles and dislocation loops. So the total increase in yield strength $\Delta\sigma_{totaly}$ can be expressed as:

$$\Delta\sigma_{totaly} = \sqrt{\sigma_{He}{}^2 + \sigma_{Loop}{}^2} \quad (3)$$

According to Eqs. (2) and (3), the yield strength increment of original sample caused by dislocation loop and helium bubble is 1716 and 497 MPa. The total yield strength increment is 1786 MPa. It can be seen that the irradiation hardening caused by dislocation loop is obvious. For the annealed sample, the yield strength increment caused by dislocation loop and helium bubble is 2166 and 53 MPa, and the total is 2167 MPa. The irradiation hardening caused by dislocation loop is more obvious than that caused by helium bubble.

Although dislocation loops and helium bubbles are generated in both

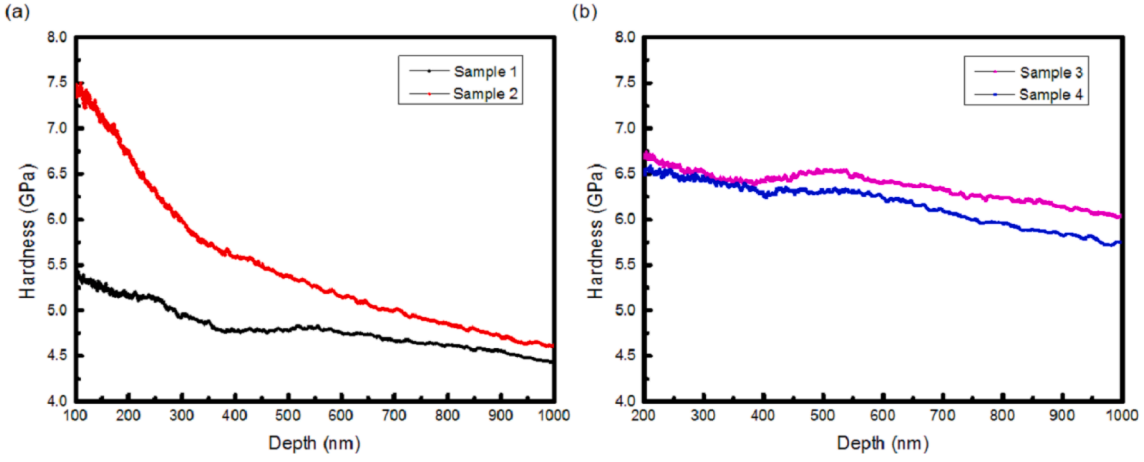

Fig. 1. Nanohardness versus indentation depth curves of the original alloys and (b) the annealed alloys before and after irradition.

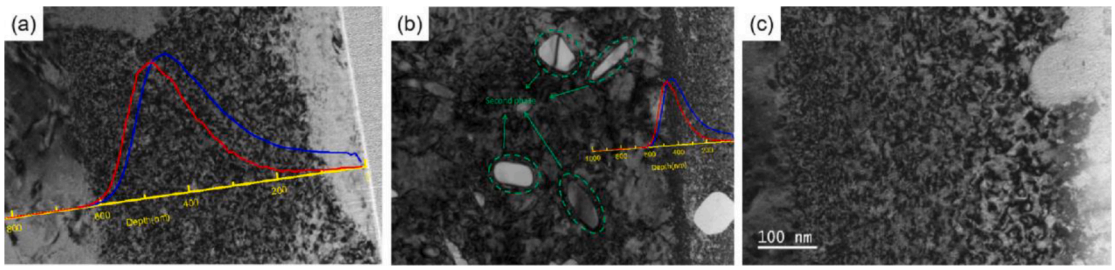

Fig. 2. (a) Dislocation loops in the original alloys; (b) and (c) dislocation loops in the annealing alloys.

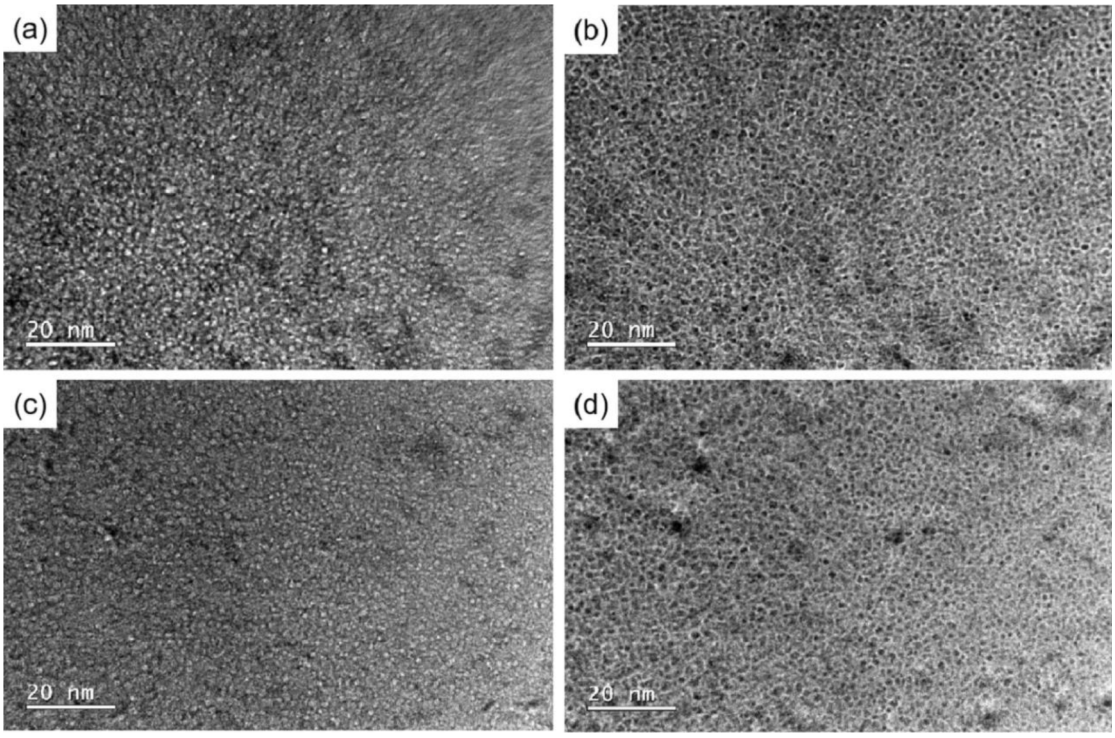

Fig. 3. (a), (b) Helium bubbles in original alloys ; (c), (d) helium bubbles in annealed alloys.

the irradiated original sample and the annealed sample, it can be concluded from the above data analysis that the irradiation hardening phenomenon occurs in the original sample, but not in the annealed sample. This is because the annealing treatment introduces many second phases into the sample, as shown in the green circle in Fig. 2(b), with a size of 100–200 nm, The existence of the second phases inhibit the occurrence of irradiation hardening phenomenon and reduce the irradiation damage. Therefore, annealing treatment improves the irradiation resistance of FeCoNiAlTi high entropy alloys.

4. Conclusion

The radiation hardening phenomenon occurred in the original alloys after irradiating by He^+ ion. The second phase is introduced into annealing treatment to effectively improve the strength and hardness of alloys. Duloop He^+ ion implantated, the irradiation resistance of alloys can be significantly improved. The average number densities of dislocation loops in the original alloys and annealed alloys were 1.38×10^{22} m^{-3} and 2.77×10^{22} m^{-3} respectively, while the average bubble sizes were 13.83 and 10.96 nm. Meanwhile, the average number densities of Helium bubbles in two materials were 9.6×10^{23} m^{-3} and 1.45×10^{24} m^{-3} when the average sizes were 1.67 and 1.25 nm.

CRediT authorship contribution statement

Han Li: Methodology, Validation, Writing – original draft. **Yongkun Mu:** Investigation, Formal analysis, Writing – review & editing. **Gang Wang:** Formal analysis, Writing – review & editing. **Yandong Jia:** Formal analysis, Writing – review & editing. **Runzhong Wang:** Methodology.

Declaration of Competing Interest

The authors declare that they have no known competing financial interests or personal relationships that could have appeared to influence the work reported in this paper.

Acknowledgements

This work is supported by the open research fund of Songshan Lake Materials Laboratory (no. 2021SLABFN06), the Innovation Program of Shanghai Municipal Education Commission (no. 2021-01-07-00-09-E00114), the financial support from Program 173 (no. 2020-JCIQ-ZD-186-01) and the National Natural Science Foundation of China (Grant numbers 51971123, 51925103, 51827801, 51801027).

References

[1] M.C. Troparevsky, J.R. Morris, M. Daene, et al., JOM. 67 (2015) 2350–2363.
[2] M.H. Chuang, M.H. Tsai, W.R. Wang, et al., Acta. Mater. 59 (2011) 6308–6317.
[3] Y.P. Lu, Y. Dong, S. Guo, et al., Sci. Rep. 4 (2014) 6200.
[4] D.S. Aidhy, C. Lu, K. Jin, et al., Acta. Mater. 99 (2015) 69–76.
[5] I. Kunce, M. Polanski, K. Karczewski, et al., J. Alloys Compd. 648 (2015) 751–758.
[6] H. Shiratori, T. Fujieda, K. Yamanaka, et al., Mater. Sci. Eng. 656 (2016) 39–46.
[7] Z. Liu, W. Zhou, Y. Lu, et al., Mater. Lett. 225 (2018) 85–88.
[8] W. Nix, H. Gao, J. Mech. Phys. Solids. 46 (1998) 411–425.
[9] H.C. Chen, R.D. Lui, C.L. Ren, et al., J. Appl. Phys. 120 (2016) 125–303.
[10] H. Trinkaus, B.N. Singh, J. Nucl. Mater. 323 (2003) 2–3.
[11] S.J. Zhang, D.H. Li, H.C. Chen, et al., J. Nucl. Mater. 489 (2017) 180–186.
[12] J.Z. Liu, H.F. Huang, J. Gao, et al., J. Nucl. Mater. 517 (2019) 328–336.